Comparing the Performance of FLUFF-BALL to SEAL-CoMFA with a Large Diverse Estrogen Data Set: From Relevant Superpositions to Solid Predictions

Samuli-Petrus Korhonen,* Kari Tuppurainen, Reino Laatikainen, and Mikael Peräkylä

Department of Chemistry, University of Kuopio, P.O. Box 1627, FIN-70211, Kuopio, Finland

Received January 21, 2005

In this work a template-based molecular mechanistic superposition algorithm FLUFF (Flexible Ligand Unified Force Field) and an accompanying local coordinate QSAR method BALL (Boundless Adaptive Localized Ligand) are validated against the benchmark techniques SEAL (Steric and Electrostatic Alignment) and CoMFA (Comparative Molecular Field Analysis) using a large diverse set of 245 xenoestrogens extracted from the EDKB (Endocrine Disruptor Knowledge Base) maintained by NCTR (National Centre for Toxicological Research). The results indicate that FLUFF is capable of generating relevant superpositions not only for BALL but also for CoMFA, as both techniques give predictive QSAR models. When the BALL and CoMFA methods are compared, it is clear that the BALL algorithm met or even exceeded the results of the standard 3D-QSAR method CoMFA using alignments either from the tailor-made superposition technique FLUFF or the reference method SEAL. The FLUFF-BALL method can be easily automated, and it is computationally light, providing thus a good computational "sieve" capable of fast screening of large molecule libraries.

1. INTRODUCTION

When faced with a challenging task of screening large libraries of molecules for biological activity, be it for drug discovery or for identification of possible endocrine disruptors, the benefits of virtual screening with quantitative structure activity relationship (QSAR) techniques become immediately obvious. Instead of arduous and expensive laboratory work the biological activity could be predicted with a suitable QSAR technique which only requires computing capacity. Alternatively, if the structure of the binding site on receptor or enzyme is known it is possible to use ligand docking techniques[1−4] to predict binding orientation[5,6] and affinity[1,7] of the ligands. For further details on ligand docking the reader is referred to recent reviews by Krovat et al.[3] and Taylor et al.[4] The great promise of the in silico techniques has led to a veritable explosion in the number of QSAR algorithms available. Unfortunately, the activity data generated from a QSAR analysis is usually far from perfect, and despite intensive efforts there is no universal solution for the structure-based prediction of the biological activity for a diverse set of compounds. The automatization of the QSAR analysis has also proven to be most elusive.[8−11]

The classical QSAR[12] relies on topological or 2D-representations of molecules, and therefore it neglects a considerable amount of stereochemical information. This has led to the development of 3D-QSAR methods such as CoMFA[13] and GRIND[14] among others.[15−27] Although the 3D-QSAR techniques are generally considered to be the most effective means of predicting the biological activity, they usually require an accurate superposition of structures, which has proven to be the major bottleneck.[8,10,11,28,29] The alignment procedure often requires considerable human intervention, and it is generally the most time-consuming phase of the 3D-QSAR analysis.[14] Despite intense efforts and semiautomated solutions such as QXP,[30] SEAL,[31] and many others,[28,32−51] the superposition remains a problem for the 3D-QSAR techniques, limiting severely their efficiency when dealing with large libraries of molecules. Melani et al.[28] have compiled an extensive summary of the different superposition algorithms available. A large number of QSAR techniques[14,23,52−64] circumvent the superposition problem by using QSAR descriptors which could be called "21/2-dimensional" as they are sensitive to the 3D-structure of the molecule, but they do not directly depend on the 3D-structure.[14,65] However, the descriptors and the results of the models are often more difficult to interpret than in the case of 3D-QSAR techniques.[14]

In this paper, a template-based grid-independent QSAR method BALL (Boundless Adaptive Localized Ligand)[66] and an accompanying superposition method FLUFF (Flexible Ligand Unified Force Field)[66] are validated using a large and highly diverse set of xenoestrogens, i.e., organic compounds that interfere with the normal function of the estrogen receptor (ER) causing thus a potential environmental risk. For reliable validation, it is vital that the same data set is processed using well-established superposition and QSAR techniques in order to evaluate the relative performance of FLUFF-BALL. The QSAR models obtained for the xenoestrogens with FLUFF-BALL are compared here with the benchmark model generated by CoMFA[13] and SEAL[31] methods. Furthermore, mixed models are generated using FLUFF superpositions as an input for CoMFA and, conversely, the SEAL superposition as an input for the BALL in order to ascertain how tightly the superposition and QSAR technique pairs are linked together. For validation purposes, the FLUFF superposition and BALL QSAR parameters are optimized using an exhaustive search methodology. In

* Corresponding author phone: +358-17-163275; fax: +358-17-163259; e-mail: Samuli-Petrus.Korhonen@uku.fi.

10.1021/ci050021i CCC: $30.25
Published on Web 10/18/2005

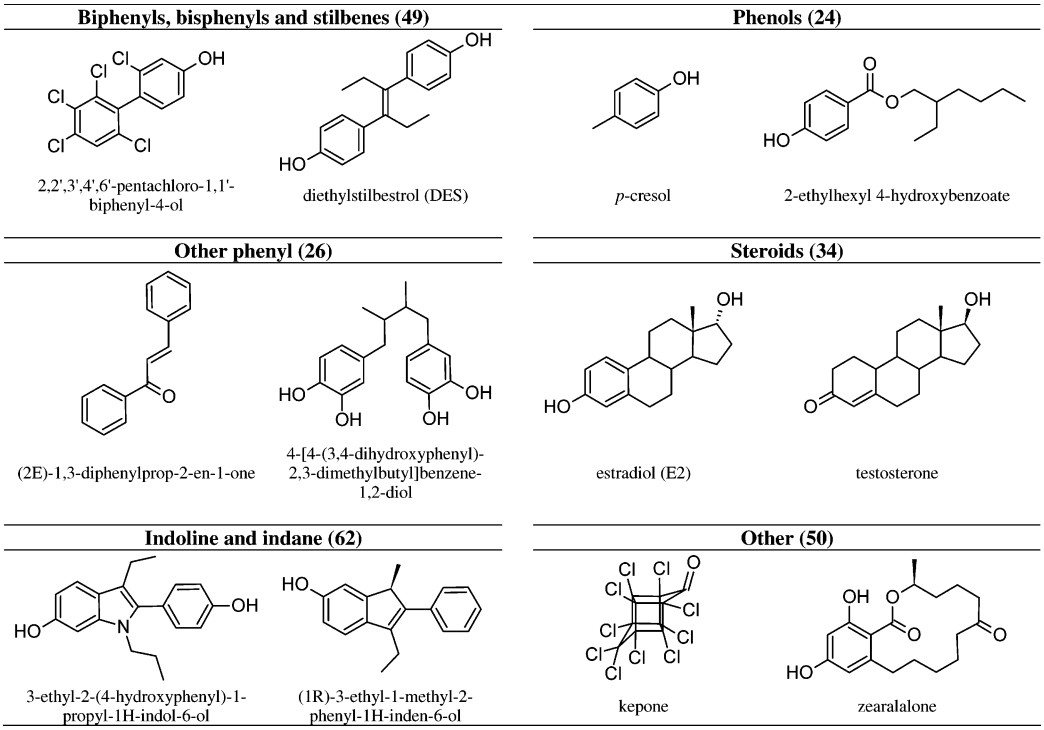

Figure 1. Structural categories and some example structures of the compounds filtered from the EDKB database. The number of compounds in each category is given in parentheses.

standard use this kind of procedure would not be necessary, but when validating a recently developed technique, it is vital that the performance limits of the technique are thoroughly evaluated. In contrast, no parameter optimization was performed for SEAL and CoMFA as they were used in this work as reference techniques, primarily to establish a baseline predictive ability for the xenoestrogen data set used in this work. Also, both SEAL and CoMFA are well-established techniques whose behavior and optimal parameters have been mapped out over years and numerous applications. On the other hand, the FLUFF-BALL is a new technique, and its behavior and optimal parameters are unknown at this time.

2. EXPERIMENTAL DATA

The estrogen binding affinities used in this work were obtained from a freely available stand-alone version of the endocrine disruptor knowledge base (EDKB, http://edkb.fda.gov) maintained by National Centre for Toxicological Research (NCTR). The EDKB contains about 2000 molecules, many of which do not bind to the ER, rendering the whole of EDKB as such useless as a QSAR benchmark set. Therefore the following selection criteria were used to filter a subset of the EDKB for this work: (1) a molecule must have an experimental binding affinity data present, (2) a molecule must have detectable binding affinity to ER, and (3) a molecule should be small to medium in size. This filtering extracted a subset of 245 molecules containing experimental data for five different estrogen receptors. For further information about the 245 compounds selected, see Figure 1. For detailed structures and biological activities (relative binding affinities, RBA values), the reader is referred to a previous publication.[67] As some molecules contained experimental values for several receptors there were a total of 374 log RBA values present for 245 molecules. In cases where several RBA values for the same receptor were present in the EDKB, the same experimental source was preferred as far as possible. Each estrogen receptor type was treated as a separate data set yielding five evenly distributed sets of experimental values (Table 1).

Table 1. EDKB Data Sets Used in This Work

receptor	molecules	average log RBA (min − max)
CALF	53	0.40 (−2.00−2.00)
HUMANA	61	−0.05 (−2.00−2.48)
HUMANB	61	0.05 (−2.00−2.61)
MOUSE	69	0.00 (−3.36−2.94)
RAT	130	−1.42 (−4.50−2.60)

The molecules were built using the HYPERCHEM program (version 4.5, http://www.hypercube.com) and subsequently optimized using the AM1 Hamiltonian as implemented in the AMPAC program (version 2.1, QCPE#506). After optimization the structures were verified by hand to ensure that all configurations had been correctly assigned and that the molecules had adopted relaxed conformations.

3. COMPUTATIONAL METHODS

3.1. Superposition. The structures of each of the five subsets were imported to an in-house developed MMS program (a modified version based on R2004.07, http://www.perchsolutions.com) so that the AM1 optimized coordinates and charges were preserved. After importing the molecules were centered according to their centers of mass. Estradiol-17β (E2, Figure 2) was imported as a template molecule, required by the FLUFF and SEAL superposition algorithms. Then the compounds were initially superimposed using a rigid FLUFF superposition on the aromatic ring (marked A in Figure 2) of the template.

3.1.1. FLUFF Superposition. FLUFF[66] is a superimposition force field based on a modified Merck Molecular Force Field (MMFF94)[68−72] easily tunable by adjusting the param-

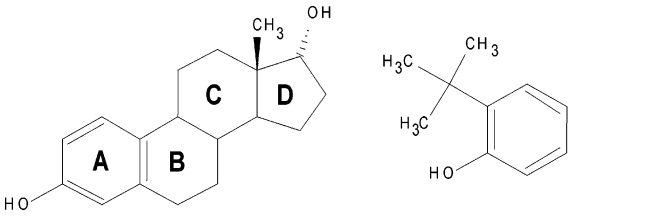

Estradiol **EDKB001 (2-*tert*-butylphenol)**

Figure 2. The structures of the template and the first ligand EKDB001.

eters for each atom type. It is also possible to include repulsive terms in order to incorporate *not-like-that* type of "negative" superposition rules. The force field nature of FLUFF means that it can utilize well-documented and tested computational techniques available for the standard molecular mechanics force fields. The actual superimposition is usually accomplished by performing a geometry optimization by using the superimposition force field. Alternatively, molecular dynamics (MD) or Monte Carlo search (MC) can be utilized.

For the FLUFF algorithm we have defined the concepts of physical and logical molecules. The physical molecule is defined as a collection of atoms interconnected by bonds. Logical molecules may consist of one or more physical molecules, parts of physical molecule(s), or they may even be an arbitrary collection of atoms. The template and ligand(s) used in FLUFF superposition are logical molecules. In the FLUFF force field the bonded and the nonbonded MMFF94 terms are generated normally within a logical molecule, whereas between logical molecules the nonbonded part is omitted. Instead, a term is added describing the van der Waals and electrostatic similarity of the ligand and the template using a Gaussian type functions (e^{x^n}) which are also used in the SEAL[31] superposition algorithm. For full technical details of the FLUFF algorithm please refer to the original article.[66] The current implementation of the FLUFF superposition algorithm provides three main variants, **FIX**, **MIX**, and **FLEX**, all of which were utilized in this work (Figure 3). The **FIX** superposition sets were created using a rigid superposition algorithm where rigid ligand is superimposed on a stationary template using FLUFF force-field and standard energy minimization procedure, whereas in the **MIX** set the ligands were fully flexible, but the template was rigid. In the **FLEX** set both the template and ligand were fully flexible and could thus adapt their conformations according to the FLUFF field and seek the best common conformation.

For FLUFF superposition the tentatively superimposed set was modified by including or excluding the methyl group (C18, attached to C13) from the estradiol-17β template thus creating **CI** and **CE** sets, respectively (Figure 3). This was done as trial superposition runs indicated that in some cases the methyl group hinders the matching of the backbone atoms. Further sets were generated by exclusion of the hydrogen atoms from the FLUFF field during the superposition, thus creating the **EH** sets. This was done in order to eliminate the barrier effect, which could also hinder the backbone superposition. After the initial superposition without hydrogen atoms, the **IH** sets were generated by including the hydrogen atoms in the FLUFF field and performing a full superposition using the **EH** set as an initial guess.

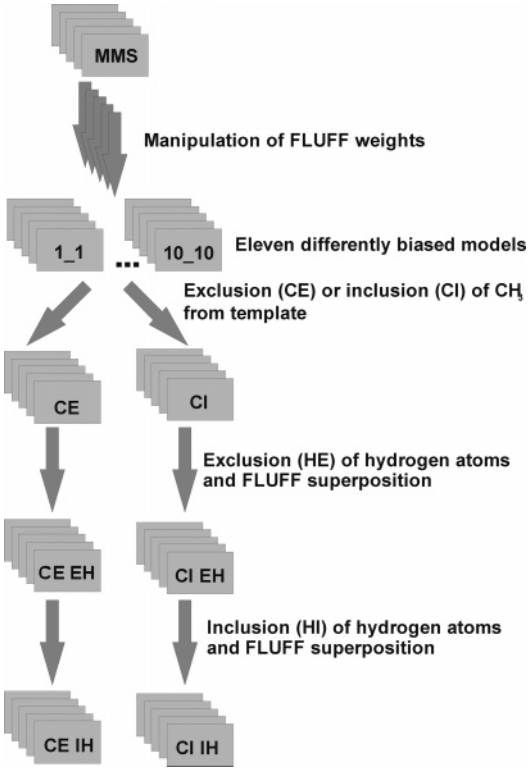

Figure 3. Flowchart of the FLUFF superposition and the creation of the different data sets.

Thus for each of the five experimental data sets a total of 12 different FLUFF models were generated. However, it soon became apparent that the EDKB data set is too diverse to be unambiguously superimposed without any a priori information. This can be easily demonstrated using the template and the first ligand EDKB001 (Figure 2). As can be seen there is no unique alignment for the EDKB001, if the only criteria used were the steric and electrostatic properties of the molecules. The EDKB001 can be placed upon the *A* ring of the template in many different orientations, but the aromatic ring of the EDKB001 can also be matched to *B*, *C*, or even to the *D* ring of the template as well. Therefore, additional information about the relative importance of the different molecular features of the template is required. As FLUFF is in essence a special molecular mechanics force field, the atom types could be used to provide additional information. However, trial runs performed using other data sets[21] have indicated that this kind of selectivity works well only in cases where the molecules are fairly similar. Unfortunately, this is not the case with the EDKB data, and other constraints for guiding the superposition must be used. The current implementation of FLUFF enables the user to assign arbitrary weight factors for the template and ligand atoms and thus increase the amount of information available to the superposition algorithm. In this case several previous QSAR works[56,73−77] suggested that for estradiol-17β the aromatic *A* ring and the hydroxyl group attached to it are important for the biological activity. Therefore the *A* ring of the template was selected as the target for the weight factor modifications, and 11 different weight factor combinations were generated (Table 2).

The **1_1** set corresponds to the unbiased superposition, and the set **10_10** leads to a superposition where the *A* ring has roughly equal weight as the remaining part of the

Table 2. Names and Weight Factors of the 11 FLUFF Models Used To Test the Effect of the Directed Superposition

name	A ring OH weight	A ring weight
1_1	1.0	1.0
2_2	2.0	2.0
3_2	3.0	2.0
3_3	3.0	3.0
4_2	4.0	2.0
4_4	4.0	4.0
5_2	5.0	2.0
5_5	5.0	4.0
10_2	10.0	2.0
10_5	10.0	5.0
10_10	10.0	10.0

molecule. Some trials were also done using weight factors up to 25, but they led to models where the *A* ring was overly dominant and caused the ligands to spread out in a fanlike formation. These heavily biased superpositions yielded inferior QSAR models, and so they were discarded.

3.1.2. SEAL Superposition. SEAL superposition was performed by using an in-house SPL script in conjunction with a TRIPOS SPL script (seal.spl as distributed with the SYBYL program, version 6.9.1) and the SEAL program (QCPE #634). To import the molecular structures to the SYBYL program (version 6.9.1, http://www.tripos.com), the tentative superposition was exported from MMS program as MDL MOL-files, which were converted to the TRIPOS MOL2 -format with the OpenBabel program (version 1.100.2, http://openbabel.sourceforge.net). The MOL2-files were used to generate a SYBYL molecular database, in which the SEAL superposition was performed. All optional parameters were set at the default values present in the TRIPOS script file.

3.2. QSAR. 3.2.1. BALL. The name Boundless Adaptive Localized Ligand (BALL) indicates all the major features of this QSAR methodology. It uses a template structure, which is given as a logical molecule (see section 3.1.1), to create a very sparse localized grid tied to centers of the template atoms. This enables the BALL grid to adapt by deforming as the template changes its conformation. The ligands are described with soft functions, such as Gaussian primitives and electrostatic potential, so that the molecule does not end abruptly but rather becomes fuzzy and slowly fades away. The current implementation of the BALL model is based on two different functions. The first one describes the van der Waals similarity of the template and ligand molecules by generating three terms based on the Gaussian primitives describing (1) the template atom's own volume by self-overlap, (2) the common volume of the template atom and ligand atoms, and (3) the residual ligand volume allocated to the template atom. The second function reflects the similarity of charges in the molecules by generating three electrostatic terms representing (1) the template's electrostatic field at the center of the template atom, (2) the difference of template's and ligand's electrostatic fields at the center of the template atom, and (3) the residual field difference allocated from ligand atoms. Thus the complete descriptor consists of 6*n* terms, where *n* is the number of template atoms. The terms describing the template atom's own volume and the electrostatic field at the center of the template atom are included primarily for scaling purposes. For full technical details of the BALL algorithm please refer to the original article.[66]

After the evaluation of the BALL descriptors the actual QSAR model may be built using arbitrary statistical analysis methodology. To further analyze the observed structure−activity relationships it is possible to back-project the QSAR model onto the template molecule from which the descriptors were evaluated. However, the very sparse BALL grid tied to the centers of template atoms is not directly suitable for creation of (interaction energy) contour maps. On the other hand, the BALL grid is directly linked to the template structure, and therefore it can be used to directly estimate the importance of different sites in the template molecule. It is also possible to use a suitable decay function to create a dense CoMFA style grid from the sparse BALL grid and then create standard contour maps. However, one should note that beyond the template structure the BALL descriptors, and therefore also the BALL results, will become fuzzy. After a while the BALL results will average out, and the contour map will become meaningless.

BALL algorithm requires four user-defined parameters. The first two parameters are VdW_const and VdW_radius-Intensity, which control the behavior of the van der Waals similarity function. The last two, VdW_dispersion and EEL_dispersion, control the allocation of "orphan" van der Waals and electrostatic density to the template atoms. Although some knowledge of the optimal BALL parameters[66] exists, it was decided that the full optimization procedure should be performed in order to evaluate the stability of the BALL model in detail. The value of vdW_const was set at one in all validation runs because earlier testing had indicated that no scaling is actually needed. For vdW_radiusIntensity, the values 0.950, 0.900, 0.850, 0.800 0.750, 0.700, 0.650, 0.600, 0.550, 0.500, 0.250, 0.125, 0.075, 0.050, and 0.025 were evaluated. For vdW_dispersion and EEL_dispersion, the values 0.500, 0.250, 0.125, 0.075, and 0.050 were evaluated. Altogether, this yields a total of 375 different combinations of parameters.

3.2.2. CoMFA. The CoMFA descriptors were evaluated using SYBYL and an in-house SPL script. Using an automatically generated region, standard CoMFA fields containing both steric and electrostatic interactions were generated using a standard distance decay ($1/r^2$) for the computation of dielectric terms, no smoothing, and a 30.0 kcal/mol cutoff with smooth transition for both steric and electrostatic energy terms. For statistical analysis the CoMFA descriptors were exported as text files from SYBYL using an in-house SPL script.

3.3. Statistical Methods. For the model building phase of PLS analyses, the following abbreviations are used throughout this paper: CV = cross-validation, LOO = leave-one-out, PRESS = predictive residual sum of squares, S_{PRESS} = cross-validated standard error of prediction (eq 1), and Q^2 = cross-validated correlation coefficient (eq 2)

$$S_{\mathrm{PRESS}} = \sqrt{\frac{\mathrm{PRESS}}{n-c-1}} \tag{1}$$

$$Q^2 = 1 - \frac{\sum(y_{\mathrm{obs}} - y_{\mathrm{pred}})^2}{\sum(y_{\mathrm{obs}} - y_{\mathrm{mean}})^2} = 1 - \frac{\mathrm{PRESS}}{\sum(y_{\mathrm{obs}} - y_{\mathrm{mean}})^2} \tag{2}$$

where *n* is the number of compounds and *c* is the number of the principal components extracted, i.e., the S_{PRESS} value is

Table 3. *CALF* Internal Validation Results

			S_{PRESS}	Q^2	NPC	R^2	F	vdW_RI	vdW_D	EEL_D
FLUFF	BALL	FIX	0.718−0.788	0.431−0.433	8−15	0.826−0.966	26.1−59.0	0.700−0.750	0.050−0.075	0.050−0.250
		FLEX	0.622−0.718	0.518−0.695	8−15	0.841−0.980	29.1−72.9	0.650−0.800	0.050−0.250	0.050−0.250
		MIX	0.465−0.682	0.610−0.824	15	0.957−0.976	45.9−65.8	0.650−0.750	0.50−0.500	0.050−0.500
FLUFF	CoMFA	FIX	0.730−0.915	0.405−0.502	11−15	0.967−0.999	109.7−861.3			
		FLEX	0.680−0.683	0.502−0.530	10−12	0.976−0.980	160.5−167.6			
		MIX	0.675−0.794	0.489−0.530	10−15	0.974−0.994	154.9−258.4			
SEAL	BALL		0.875	0.223	12	0.312	30.5	0.750	0.500	0.050
SEAL	CoMFA		0.887	0.117	1	0.864	8.0			

Table 4. *HUMANA* Internal Validation Results

			S_{PRESS}	Q^2	NPC	R^2	F	vdW_RI	vdW_D	EEL_D
FLUFF	BALL	FIX	0.900−1.149	0.577−0.761	13−15	0.974−0.996	96.4−362.3	0.750−0.850	0.120−0.500	0.050−0.500
		FLEX	0.985−1.245	0.478−0.656	11−15	0.970−0.993	144.7−290.2	0.650−0.750	0.500	0.050−0.120
		MIX	1.024−1.209	0.569−0.678	13−15	0.984−0.999	226.8−1622.8	0.550−0.750	0.050−0.500	0.120−0.250
FLUFF	CoMFA	FIX	1.131−1.481	0.353−0.407	2−15	0.609−1.000	45.1−7191.3			
		FLEX	1.148−1.216	0.294−0.400	3−6	0.728−0.935	50.8−129.9			
		MIX	1.189−1.231	0.289−0.333	2−5	0.513−0.915	30.6−118.0			
SEAL	BALL		1.378	0.375	15	0.998	852.7	0.650	0.120	0.500
SEAL	CoMFA		1.384	0.163	2	0.461	24.8			

Table 5. *HUMANB* Internal Validation Results

			S_{PRESS}	Q^2	NPC	R^2	F	vdW_RI	vdW_D	EEL_D
FLUFF	BALL	FIX	1.019−1.049	0.398−0.606	4−15	0.658−0.991	33.6−186.9	0.650−0.750	0.500	0.050−0.500
		FLEX	1.026−1.345	0.382−0.486	10−15	0.954−0.997	103.3−471.8	0.650−0.750	0.500	0.050−0.500
		MIX	1.137−1.213	0.397−0.533	13−15	0.971−0.993	119.3−347.4	0.025−0.750	0.250−0.500	0.120−0.500
FLUFF	CoMFA	FIX	1.102−1.392	0.313−0.338	3−15	0.706−1.000	45.7−4092.5			
		FLEX	1.078−1.445	0.286−0.376	3−15	0.770−1.000	63.8−27537.5			
		MIX	1.072−1.147	0.281−0.383	2−5	0.529−0.901	32.6−100.6			
SEAL	BALL		1.039	0.410	4	0.801	56.3	0.700	0.120	0.050
SEAL	CoMFA		1.272	0.279	8	0.965	177.8			

weighted so that it penalizes models with a high number of principal components. For fitted models, R^2 = squared correlation coefficient, SE = standard error, and F = Fischer test for significance. For external test sets R_{ex}^2 = squared correlation coefficient, $|\Delta_{av}|$ = mean absolute deviations, Pr-R^2 = predictive R^2-score (eq 3), and SDEP = standard error of prediction (eq 4)

$$\text{Pr-}R^2 = \frac{\text{SD} - \text{PRESS}}{\text{SD}} \tag{3}$$

$$\text{SDEP} = \sqrt{\frac{\text{PRESS}}{n}} \tag{4}$$

where SD is the sum of squared deviations between the activities of molecules in the test set and the mean affinity of the training set molecules.

4. RESULTS AND DISCUSSION

The QSAR models were generated with PLS method and LOO-CV using MATLAB (version 6.5, The MathWorks Inc., http://www.mathworks.com) scripts. The maximum number of principal components (PC) was set at 15 based on the generally accepted one-quarter rule, i.e., the number of PCs should not exceed $n/4$, where n is the number of molecules. For the *RAT* set the maximum number of principal components could be as high as 32 and still conform to the one-quarter rule. Therefore additional PLS models with the maximum number of principal components set at 25 and 30 were generated. Some increase in the Q^2 values were observed, but the benefits were negligible (<0.050), and the number of components rose dramatically, being in the range of 25−28. Therefore it was judged that the gains made in the Q^2 values did not outweigh the dramatic increase in the number of principal components and these models were discarded.

For each of the five data sets there were originally 49 875 BALL models and 133 CoMFA models. Therefore the results are "distilled" so that only the information necessary to support the conclusions are presented in this paper. (If someone is interested in the raw data, the Excel files containing the full results are available upon a request from the corresponding author.) For each superposition the optimum BALL model (**FIX**, **FLEX**, and **MIX** with **CE**/**CI** and **EH**/**IH** modifications) was selected for further analysis using the maximum Q^2 value. The 133 remaining BALL and CoMFA models were filtered further by selecting the optimum FLUFF weight factors based on the maximum Q^2 value achieved, thus reducing the 132 FLUFF superpositions down to 12. In the summarized results for the five data sets (Tables 3−7) only the reference set generated using SEAL and range of descriptors yielded by the **CE**/**CI** and **EH**/**IH** sets is shown thus reducing the number of FLUFF QSAR models down to 3 for both BALL and CoMFA. This was done as the effect of the modifications was minor. However, replacement tables, showing 12 FLUFF superpositions are available as Supporting Information.

4.1. Effect of Superposition. When different FLUFF superpositions are compared, it is evident that no clear optima can be found, and therefore it is difficult to discern the optimal FLUFF variant between the **FIX**, **FLEX**, and **MIX**. If only the best models of each data set are compared for

Table 6. *MOUSE* Internal Validation Results

			S_{PRESS}	Q^2	NPC	R^2	F	vdW_RI	vdW_D	EEL_D
FLUFF	BALL	FIX	1.154−1.270	0.476−0.611	9−15	0.871−0.905	32.5−50.5	0.250−0.550	0.250−0.500	0.075−0.250
		FLEX	1.195−1.282	0.438−0.512	6−7	0.771−0.808	34.8−37.9	0.850−0.900	0.050−0.500	0.250−0.500
		MIX	1.197−1.251	0.431−0.519	2−7	0.543−0.803	35.2−39.2	0.700−0.850	0.050−0.250	0.050−0.120
FLUFF	CoMFA	FIX	1.232−1.303	0.410−0.482	5−6	0.899−0.941	111.8−140.6			
		FLEX	1.312−1.362	0.325−0.374	2−4	0.544−0.883	39.4−120.9			
		MIX	1.337−1.344	0.353−0.427	3−10	0.702−0.986	51.0−396.2			
SEAL	BALL		1.345	0.362	4	0.635	27.9	0.500	0.050	0.075
SEAL	CoMFA		1.592	0.178	2	0.464	28.6			

Table 7. *RAT* Internal Validation Results

			S_{PRESS}	Q^2	NPC	R^2	F	vdW_RI	vdW_D	EEL_D
FLUFF	BALL	FIX	1.257−1.334	0.470−0.533	7−8	0.719−0.776	44.4−52.3	0.800−0.850	0.250−0.500	0.050−0.250
		FLEX	1.262−1.396	0.452−0.529	7−15	0.736−0.914	48.7−71.9	0.700−0.850	0.120−0.500	0.120−0.500
		MIX	1.243−1.367	0.490−0.547	7−15	0.690−0.962	52.5−109.7	0.800−0.850	0.120−0.500	0.075−0.500
FLUFF	CoMFA	FIX	1.060−1.174	0.582−0.673	5−10	0.867−0.963	161.4−313.5			
		FLEX	1.245−1.337	0.445−0.545	5−11	0.846−0.967	135.8−313.8			
		MIX	1.226−1.332	0.463−0.546	4−12	0.824−0.977	134.6−415.6			
SEAL	BALL		1.419	0.385	4	0.583	43.7	0.600	0.050	0.250
SEAL	CoMFA		1.743	0.157	2	0.351	34.4			

both BALL and CoMFA, it appeared that 3 out of 5 models are generated using the **FIX** method. On the other hand, taking the best 6 of the models for each data set and making a similar analysis no such trend is observed. If the optimal FLUFF variant is difficult to discern, the optimal weight factors proved to be even more elusive as all available weight factor combinations are present among the optimal models generated for BALL and CoMFA. In fact, the only clear pattern was observed in the *CALF* data set, in which 7 out of 12 FLUFF superpositions used the weight parameter set **5_2**. In general, medium weight factors seem to be optimal, although there are some models that clearly prefer strict constraints. In general, it seems that BALL prefers stricter constraints than CoMFA.

The primary reason for the fact that no clear optima could be found for the FLUFF superposition parameters was that the QSAR models form a large plateau of good predictive ability where the relative differences in the performance of the QSAR are very small. Furthermore, this plateau is dotted with models of higher predictive ability which, however, do not form any clear pattern. It seems that a good QSAR model can be derived from a wide variety of FLUFF superpositions, and the optimal models are scattered onto a plateau of good performance. This is in agreement with the well-known fact that the 3D-QSAR is highly sensitive to the superposition.[9,73,78] Therefore one must conclude that the choice of FLUFF superposition and the use of a priori information in the form of weight factors must be decided on case-by-case basis, and no universal guidelines can be given at this time.

However, a clear difference in performance can be observed between SEAL and FLUFF. Of course, one should bear in mind that the SEAL superposition is only an unoptimized benchmark, but even then the difference between FLUFF and SEAL is significant. This difference could be caused by the force-field nature of the FLUFF technique as it has the ability of providing additional information about the bond patterns and the neighbors of an atom through the use of molecular mechanical atom types that contain this information implicitly. A possible explanation for the superior performance of the FLUFF algorithm is also the fact that it has additional a priori information about the relative importance of the features of the template in the form of the user-specified weight factors. The fact that the differences between the **FIX**, **FLEX**, and **MIX** variants were smaller than the differences between weight factors suggest that this a priori information plays an important role in determining the efficacy of the superposition.

Table 8. Maximum Q^2 Values Achieved in LOO CV for All Data Sets and Superposition-QSAR Pairs

	CALF	*HUMANA*	*HUMANB*	*MOUSE*	*RAT*
FLUFF-BALL	0.824	0.761	0.606	0.611	0.547
FLUFF-CoMFA	0.530	0.407	0.383	0.482	0.673
SEAL-BALL	0.223	0.375	0.410	0.362	0.385
SEAL-CoMFA	0.117	0.163	0.279	0.178	0.157

4.2. QSAR. It seems obvious that the unoptimized reference technique SEAL produces an inferior superposition compared to FLUFF, as indicated by the lower S_{PRESS} and higher Q^2 values of both FLUFF-BALL and FLUFF-CoMFA (Tables 3−8). In particular, the SEAL-CoMFA combination seems to be particularly problematic as it generates a reasonable model only for the *HUMANB* data set. The SEAL-BALL combination performs clearly better, but it still produces inferior results when compared with FLUFF. In general, BALL produces better models than CoMFA for both FLUFF and SEAL superpositions with an exception of the *RAT* data set, for which CoMFA with the FLUFF superposition yielded a slightly better model than BALL. The similar differences in predictive ability that can be observed between the optimum models generated for each data set also exists in the average results (Table 8), indicating that a real difference exists. Naturally the differences were much more marked between the optimum models.

Tropsha et al. have correctly pointed out[79] that a high Q^2 value achieved in an internal validation is only a necessary but not sufficient condition for high predictive ability. Therefore two additional statistical diagnostic tests, Y-scrambling test and external validation with separate training and test sets, were performed in order to validate the QSAR model and to assess its statistical robustness. For each of the EDKB data sets, 1000 Y-scrambling runs were performed, and in all cases the predictive ability was completely lost. For full data, please refer to Table S8 in the Supporting Information. The external validation was performed using

Table 9. *MOUSE* Internal Validation Results When VdW_RadiusIntensity Values Restricted to the Range of 0.650−0.850

			S_{PRESS}	Q^2	NPC	R^2	F	vdW_RI	vdW_D	EEL_D
FLUFF	BALL	FIX	1.203−1.275	0.459−0.482	3−10	0.605−0.965	34.9−45.6	0.650−0.800	0.050−0.120	0.075−0.120
		FLEX	1.195−1.282	0.438−0.512	6−7	0.756−0.819	34.8−37.9	0.850	0.050−0.500	0.250−0.500
		MIX	1.197−1.251	0.431−0.519	2−7	0.768−1.000	35.2−39.2	0.700−0.850	0.050−0.250	0.050−0.120

the bootstrapping methodology by creating a collection of 2500 random partitions to test/training sets consisting of 18/35, 20/41, 20/41, 23/46, and 43/87 compounds for *CALF*, *HUMANA*, *HUMANB*, *MOUSE*, and *RAT*, respectively. The results of the bootstrap runs are presented in Tables S9−S13 of Supporting Information. As expected, the statistical performance indicators worsened as a result of the bootstrapping, but all models still produced reasonable Q^2 values. The relative performance of the different superpositions changed, but usually the changes were minor and although the order may have changed, usually the same sets can still be found in the top six. However, this is not true for the *MOUSE* data set where the top three superpositions for BALL were all **FIX** sets which also produced BALL models with unusually low vdW_radiusIntensity values. When these superpositions were run through the external validation, the statistical indicators were significantly lower than those generated from other *MOUSE* sets. As a result three **MIX** sets replaced the **FIX** sets as the top three superpositions for *MOUSE* and BALL.

For the FLUFF superposition the results of the external validation of *HUMANA*, *HUMANB*, *MOUSE*, and *RAT* data sets were very similar to the results obtained from the internal validation. BALL still produced slightly better models, except for the *RAT* data set for which CoMFA still yielded better results. Here again, the differences were present in both average results and optimum models. As the overall predictive ability of the models was degraded, the differences between the models were naturally also diminished. On average the models were also predictive as indicated by positive Pr-R^2 values, but the predictive ability of the models was strongly dependent on the compounds included in the training set as can be seen from the high standard deviation (SD) values of the Pr-R^2 indicators, whereas the Q^2 values are relatively stable suggesting that the QSAR model can usually be derived successfully based on the 2/3 of compounds. The largest change from the internal validation was observed for the *CALF* data set, for which CoMFA gave slightly better average statistical indicators than BALL and even yielded the maximum Q^2 value. On the other hand, BALL generated the model with best external statistical indicators. All in all, the differences are certainly minor, but it is noteworthy that the relative predictive ability of BALL and CoMFA changed compared to the internal validation. The main reason for the poor average performance of BALL is the fact that it fails drastically for quite a few partitions of original data, whereas it works very well for all other partitions. It seems that for some reason the *CALF* data tends to create labile models that, for some randomly selected partitions, lead to a reduced performance in the internal validation and to a total loss of external predictive ability.

For the SEAL superposition, the CoMFA results are uniformly rather poor, and the negative Pr-R^2 values indicate that the models actually have no predictive ability. However, judging from the poor internal performance, this is by no means surprising. As expected, the BALL results are considerably better, even though the SEAL superposed *CALF* data set leads to relatively poor BALL models both in internal and in external validation.

When comparing the QSAR results (Tables 3−8 and Supporting Information Tables S9−S13) one should bear in mind that CoMFA was used only as a benchmark and its parameters are not optimized, but even so BALL performs remarkably well considering that its descriptor vectors consist of a few hundred elements rather than thousands, and it is thus much lighter technique than CoMFA. This implies that the BALL descriptors are faster to evaluate and much faster to process with statistical tools. This is primarily due to the design emphasis of the BALL technique, which is a grid-independent QSAR that could be easily automated for screening applications. One could also interpret the very sparse BALL grid as an extreme form of region focusing[80] where the template is used to generate a minimal grid. One possible advantage of this localized grid is the utilization of latent information about the binding site usually available in the structure of the natural ligand. Also the fuzzy nature of the BALL descriptor may be advantageous as it allows the QSAR model to describe a part of flexibility of the binding site. The lack of the 3D grid, combined with the low-dimensional descriptors, may in part explain the slight preference BALL exhibits to the strictly constrained models as the part of the ligand that falls outside the template is not evaluated using a grid, but it is allocated to the template atoms in a fuzzy manner. If the ligand is much larger than the template or it has long protruding parts, the BALL descriptor will, by design, become fuzzy for that part and lose its accuracy when compared to the grid-based descriptors. Therefore the BALL benefits from the use of heavy weight factors which forcibly align the ligands on the template thus minimizing the overspill.

4.2.1. BALL Parameters. In general, the optimal areas of the BALL parameters 0.650−0.850/0.050−0.500/0.050−0.500 (min-max vdW_radiusIntensity/min-max VdW_dispersion/min-max EEL_dispersion) found in this work are similar to the optimal areas 0.700−0.900/0.050−0.500/0.050−0.500 found in our earlier work.[66] The VdW_dispersion and EEL_dispersion parameters have a higher variance, but overall they have a lesser impact on the Q^2 value. In particular, the EEL_dispersion has only a slight effect on the predictive ability of the models as long as the compounds do not contain highly charged atoms. After a detailed analysis of the BALL models generated in this work, it became obvious that if any optimization is to be performed on the vdW_radiusIntensity parameter it should be restricted to the area of 0.650−0.850, as only seven optimal BALL models fall outside this range. Of those models, one belongs to *HUMANA*, one to *HUMANB*, and five to *MOUSE*, and actually most of them could be easily replaced with comparable models belonging to the optimum area. For the *HUMANA* data set and the FLUFF superposition **MIX CI EH**, the optimum BALL parameters are 550/500/250 (vdW_radiusIntensity/VdW_dispersion/EEL_dispersion), but

for the same superposition there is an alternative parameter set of 700/500/500, which produces only a marginally lower Q^2 value (0.675 vs 0.678). In the case of the *HUMANB* set the optimum parameters for the **MIX CE IH** superposition with weight factors 1_1 are 25/250/500, and the nearest parameter set in the optimal range is 650/250/50 with a somewhat lower Q^2 value (0.368 vs 0.401). However, if the vdW_radiusIntensity values are restricted to the range 650−850, the optimal weight factors change to 3_2, and the optimal BALL parameters are 650/500/500, yielding a Q^2 value of 0.396.

For the troublesome *MOUSE* data set a new set of optimal superpositions was generated by simply restricting the vdW_radiusIntensity parameter to the range of 0.650−0.850. The statistical indicators of the QSAR models generated from this new set of superpositions are summarized in Table 9. The restriction of the vdW_radiusIntensity caused many changes in statistical indicators, most notably the maximum Q^2 dropped from 0.611 to 0.519. However, the average Q^2 achieved suffered only a modest decrease from 0.497 to 0.475. So if the vdW_radiusIntensity is restricted to the proposed range, no great loss of performance should ensue. Based on these findings it seems clear that a focused grid search in the area of VdW_RadiusIntensity 0.650−0.850 including the two dispersion parameters should yield nearly an optimum BALL model. In terms of computational load this optimization means that 125 unique sets are to be evaluated. With a powerful desktop PC this task can be performed in less than 20 min. Furthermore this optimization can be performed without human intervention so it only demands computer time. But if the optimization is to be omitted completely, the BALL parameter set of VdW_RadiusIntensity 0.800, VdW_dispersion 0.500, and EEL_dispersion 0.500, as already proposed in our earlier work,[66] should always provide a reasonable Q^2 value.

5. CONCLUSIONS

The results of this work show that FLUFF-BALL is capable of generating robust predictive models for a large and diverse xenoestrogen data set. The **FIX**, **MIX**, and **FLEX** variants of the FLUFF superposition allowing rigid, semiflexible, and fully flexible superposition and the user-specified weight factors incorporating a priori information were successfully utilized in the superposition of a diverse xenoestrogen data set as indicated by the predictive QSAR models generated from the FLUFF data. These facts point toward the conclusion that the FLUFF method is a versatile superposition technique that is suitable not only for BALL but also for other QSAR techniques such as CoMFA. It also generated superior superpositions when compared to the reference technique SEAL. For this diverse data set BALL met or exceeded the results of the standard 3D-QSAR method CoMFA using either the tailor-made superposition technique FLUFF or the reference method SEAL. The FLUFF-BALL can easily be automated, and as it is computationally simple, it provides a good computational "sieve" capable of fast screening of large molecular libraries.

ACKNOWLEDGMENT

Samuli-Petrus Korhonen thanks The National Graduate School of Informational and Structural Biology (ISB) for financial support. Kari Tuppurainen thanks The Academy of Finland (Grant #200978). Mikael Peräkylä thanks The Academy of Finland (Grant #104622).

Supporting Information Available: Replacement tables showing 12 FLUFF superpositions. This material is available free of charge via the Internet at http://pubs.acs.org.

REFERENCES AND NOTES

(1) Oprea, T. I.; Marshall, G. R. Receptor-Based Prediction of Binding Affinities. *Perspect. Drug Discovery Des.* **1998**, *9/10/11*, 35−61.
(2) Mestres, J.; Knegtel, R. M. A. Similarity Versus Docking in 3D Virtual Screening. *Perspect. Drug Discovery Des.* **2000**, *20*, 191−207.
(3) Krovat, E. M.; Steindl, T.; Langer, T. Recent Advances in Docking and Scoring. *Curr. Comput.-Aided Drug Des.* **2005**, *1*, 93−102.
(4) Taylor, R. D.; Jewsbury, P. J.; Essex, J. W. A Review of Protein-Small Molecule Docking Methods. *J. Comput.-Aided Mol. Des.* **2002**, *16*, 151−166.
(5) De Rosa, M. C.; Berglund, A. A New Method for Predicting the Alignment of Flexible Molecules and Orienting Them in a Receptor Cleft of Know Structure. *J. Med. Chem.* **1998**, *41*, 691−698.
(6) Hare, B. J.; Walters, W. P.; Caron, P. R.; Bemis, G. W. CORES: An Automated Method for Generating Three-Dimensional Models of Protein/Ligand Complexes. *J. Med. Chem.* **2004**, *47*, 4731−4740.
(7) Goodford, P. J. A Computational Procedure for Determining Energetically Favourable Binding Sites on Biologically Important Macromolecules. *J. Med. Chem.* **1985**, *28*, 849−857.
(8) Kim, K. H.; Greco, G.; Novellino, E. A Critical Review of Recent CoMFA Applications. *Perspect. Drug Discovery Des.* **1998**, *12/13/14*, 257−315.
(9) Doweyko, A. 3D-QSAR Illusions. *J. Comput.-Aided Mol. Des.* **2004**, *18*, 587−596.
(10) Clark, D. E.; Pickett, S. D. Computational Methods for the Prediction of 'Drug-Likeness'. *Drug Discovery Today* **2000**, *5*, 49−58.
(11) Sutherland, J. J.; O'Brien, L. A.; Weaver, D. F. A Comparison of Methods for Modelling Quantitative Structure−Activity Relationships. *J. Med. Chem.* **2004**, *47*, 5541−5554.
(12) Hansch, C.; Leo, A. *Exploring QSAR: Fundamentals and Applications in Chemistry and Biology;* American Chemical Society: Washington, DC, 1995.
(13) Cramer, R. D., III.; Patterson, D. E.; Bunce, J. D. Comparative Molecular Field Analysis (CoMFA). 1. Effect of Shape on Binding of Steroids to Carrier Proteins. *J. Am. Chem. Soc.* **1988**, *110*, 5959−5967.
(14) Pastor, M.; Cruciani, G.; McLay, I.; Pickett, S.; Clementi, S. GRid-INdependent Descriptors (GRIND): A Novel Class of Alignment-Independent Three-Dimensional Molecular Descriptors. *J. Med. Chem.* **2000**, *43*, 3233−3243.
(15) Wan, J.; Yang, G.; Zhan, C.-G. Quantitative Structure−Activity Relationship for Cyclic Imide Derivatives of Protoporphyrinogen Oxidase Inhibitors: A Study of Quantum Chemical Descriptors From Density Functional Theory. *J. Chem. Inf. Comput. Sci.* **2004**, *44*, 2099−2105.
(16) Pan, D.; Iyer, M.; Liu, J.; Hopfinger, A. J. Constructing Optimum Blood Brain Barrier QSAR Models Using a Combination of 4D-Molecular Similarity Measures and Cluster Analysis. *J. Chem. Inf. Comput. Sci.* **2004**, *44*, 2083−2098.
(17) Lill, M. A.; Vedani, A.; Dobler, M. Raptor: Combining Dual-Shell Representation, Induced-Fit Simulation, and Hydrophobicity Scoring in Receptor Modeling: Application Toward the Simulation of Structurally Diverse Ligand Sets. *J. Med. Chem.* **2004**, *47*, 6174−6186.
(18) Chae, C. H.; Yoo, S.-E.; Whanchul, S. Novel Receptor Surface Approach for 3D-QSAR: The Weighted Probe Interaction Energy Method. *J. Chem. Inf. Comput. Sci.* **2004**, *44*, 1774−1787.
(19) Kotani, T.; Higashiura, K. Comparative Molecular Active Site Analysis (CoMASA). 1. An Approach to Rapid Evaluation of 3D QSAR. *J. Med. Chem.* **2004**, *47*, 2732−2742.
(20) Dunn, W. J. I.; Hopfinger, A. J. 3D QSAR of Flexible Molecules Using Tensor Representation. *Perspect. Drug Discovery Des.* **1998**, *12/13/14*, 167−182.
(21) Waller, C. L. A Comparative QSAR Study Using CoMFA, HQSAR, and FRED/SKEYS Paradigms for Estrogen Receptor Binding Affinities of Structurally Diverse Compounds. *J. Chem. Inf. Comput. Sci.* **2004**, *44*, 758−765.
(22) Vedani, A. 5D-QSAR: The Key for Simulating Induced Fit. *J. Med. Chem.* **2002**, *45*, 2139−2149.
(23) Silverman, B. D.; Platt, D. E. Comparative Molecular Moment Analysis (CoMMA): 3D-QSAR Without Molecular Superposition. *J. Med. Chem.* **1996**, *39*, 2129−2140.

(24) Norinder, U. 3-D QSAR Analysis of Steroid/Protein Interactions: The Use of Difference Maps. *J. Comput.-Aided Mol. Des.* **1991**, *5*, 419−426.

(25) So, S.-S.; Karplus, M. Three-Dimensional Quantitative Structure−Activity Relationships From Molecular Similarity Matrices and Neural Networks. 1. Method and Validations. *J. Med. Chem.* **1997**, *40*, 4347−4359.

(26) Hopfinger, A. J.; Wang, S.; Tokarski, J. S.; Baiqiang, J.; Albuquerque, M.; Madhav, P. J.; Duraiswami, C. Construction of 3D-QSAR Models Using the 4D-QSAR Analysis Formalism. *J. Am. Chem. Soc.* **1997**, *119*, 10509−10524.

(27) Hasegawa, K.; Matsuoka, S.; Arakawa, M.; Funatsu, K. New Molecular Surface-Based 3D-QSAR Method Using Kohonen Neural Network and 3-Way PLS. *Comput. Chem.* **2002**, *26*, 583−589.

(28) Melani, F.; Gratteri, P.; Adamo, M.; Bonaccini, C. Field Interaction and Geometrical Ovelap: A New Simplex and Experimental Design Based Computational Procedure for Superposing Small Ligand Molecules. *J. Med. Chem.* **2003**, *46*, 1359−1371.

(29) Martin, Y. C. 3D QSAR: Current State, Scope and Limitations. *Perspect. Drug Discovery Des.* **1998**, *12/13/14*, 3−23.

(30) McMartin, C.; Bohacek, R. QXP: Powerful, Rapid Computer Algorithms for Structure-Based Drug Design. *J. Comput.-Aided Mol. Des.* **1997**, *11*, 333−344.

(31) Kearsley, S. K.; Smith, G. M. An Alternative Method for the Alignment of Molecular Structures: Maximizing Electrostatic and Steric Overlap. *Tetrahedron Comput. Methodol.* **1990**, *3*, 613−633.

(32) Arakawa, M.; Hasegawa, K.; Funatsu, K. Novel Alignment Method of Small Molecules Using the Hopfield Neural Networks. *J. Chem. Inf. Comput. Sci.* **2003**, *43*, 1390−1395.

(33) Arakawa, M.; Hasegawa, K.; Funatsu, K. Application of Novel Alignment Method of Small Molecules Using the Hopfield Neural Networks to 3D-QSAR. *J. Chem. Inf. Comput. Sci.* **2003**, *43*, 1396−1402.

(34) McMartin, C.; Bohacek, R. Flexible Matching of Test Ligands to a 3D Pharmacophore Using a Molecular Superposition Force Field: Comparison of Predicted and Experimental Conformations of Inhibitors of Three Enzymes. *J. Comput.-Aided Mol. Des.* **1995**, *9*, 237−250.

(35) Mestres, J.; Rohrer, D. C.; Maggiora, G. M. MIMIC: A Molecular-Field Matching Program Exploting Applicability of Molecular Similarity Approaches. *J. Comput. Chem.* **1997**, *18*, 934−954.

(36) Lemmen, C.; Lengauer, T. Computational Methods for the Structural Alignment of Molecules. *J. Comput.-Aided Mol. Des.* **2000**, *14*, 215−232.

(37) Thorner, D. A.; Wild, D. J.; Willett, P.; Wright, P. M. Calculation of Structural Similarity by the Alignment of Molecular Electorstatic Potentials. *Perspect. Drug Discovery Des.* **1998**, *9/10/11*, 301−320.

(38) Klebe, G.; Mietzner, T.; Weber, F. Methodological Developments and Strategies for a Fast Flexible Superposition of Drug-Sized Molecules. *J. Comput.-Aided Mol. Des.* **1999**, *13*, 35−49.

(39) Krämer, A.; Horn, H. W.; Rice, J. E. Fast 3D Molecular Superposition and Similarity Search in Databases of Flexible Molecules. *J. Comput.-Aided Mol. Des.* **2003**, *17*, 13−38.

(40) Bultinck, P.; Kuppens, T.; Gironés, X.; Carbó-Dorca, R. Quantum Similarity Superposition Algorithm (QSSA): A Consistent Scheme for Molecular Alignment and Molecular Similarity Based on Quantum Chemistry. *J. Chem. Inf. Comput. Sci.* **2003**, *43*, 1143−1150.

(41) Robinson, D. D.; Lyne, P. D.; Richards, W. G. Partial Molecular Alignment Via Local Structure Analysis. *J. Chem. Inf. Comput. Sci.* **2000**, *40*, 503−512.

(42) Raymond, J. W.; Willett, P. Maximum Common Subgraph Isomorphism Algorithms for the Matching of Chemical Structures. *J. Comput.-Aided Mol. Des.* **2002**, *16*, 521−533.

(43) Mills, J. E. J.; de Esch, I. J. P.; Perkins, T. D. J.; Dean, P. M. SLATE: A Method for the Superposition of Flexible Ligands. *J. Comput.-Aided Mol. Des.* **2001**, *15*, 81−96.

(44) Perkins, T. D. J.; Mills, J. E. J.; Dean, P. M. Molecular Surface-Volume and Property Matching to Superpose Flexible Dissimilar Molecules. *J. Comput.-Aided Mol. Des.* **1995**, *9*, 479−490.

(45) Lemmen, C.; Lengauer, T.; Klebe, G. FLEXS: A Method for Fast Flexible Ligand Superposition. *J. Med. Chem.* **1998**, *41*, 4502−4520.

(46) Berglund, A.; De Rosa, M. C.; Wold, S. Aligment of Flexible Molecules at Their Receptor Site Using 3D Descriptors and Hi-PCA. *J. Comput.-Aided Mol. Des.* **1997**, *11*, 601−612.

(47) Lemmen, C.; Zimmermann, M.; Lengauer, T. Multiple Molecular Superpositioning As an Effective Tool for Virtual Screening. *Perspect. Drug Discovery Des.* **2000**, *20*, 43−62.

(48) Good, A. C.; Richards, W. G. Explicit Calculation of 3D Molecular Similarity. *Perspect. Drug Discovery Des.* **1998**, *9/10/11*, 321−338.

(49) Gironés, X.; Carbó-Dorca, R. TGSA-Flex: Extending the Capabilities of the Topo-Geometrical Superposition Algorithm to Handle Flexible Molecules. *J. Comput. Chem.* **2004**, *25*, 153−159.

(50) Putta, S.; Eksterowicz, J.; Lemmen, C.; Stanton, R. A Novel Subshape Molecular Descriptor. *J. Chem. Inf. Comput. Sci.* **2003**, *43*, 1623−1635.

(51) Hofbauer, C.; Lohninger, H.; Aszódi, A. SURFCOMP: A Novel Graph-Based Approach to Molecular Surface Comparison. *J. Chem. Inf. Comput. Sci.* **2004**, *44*, 837−847.

(52) Broto, P.; Moreau, G.; Vandycke, C. Molecular Structures: Perception, Autocorrelation Descriptor and SAR Studies. Autocorrelation Descriptor. *Eur. J. Med. Chem.* **1984**, *19*, 66−70.

(53) Wagener, M.; Sadowski, J.; Gasteiger, J. Autocorrelation of Molecular Surface Properties for Modeling Corticosteroid Binding Globulin and Cytosolic Ah Receptor Activity by Neural Networks. *J. Am. Chem. Soc.* **1995**, *117*, 7769−7775.

(54) Bravi, G.; Gancia, E.; Mascagni, P.; Pegna, M.; Todeschini, R.; Zaliani, A. MS-WHIM, New 3D Theoretical Descriptors Derived From Molecular Surface Properties: A Comparative 3D QSAR Study in a Series of Steroids. *J. Comput.-Aided Mol. Des.* **1997**, *11*, 79−92.

(55) Silverman, B. D. The Thirty-One Benchmark Steroid Revisited: Comparative Molecular Moment Analysis (CoMMA) With Principal Component Regression. *Quant. Struct.−Act. Relat.* **2000**, *19*, 237−246.

(56) Robert, D.; Amat, L.; Carbó-Dorca, R. Three-Dimensional Quantitative Structure−Activity Relationships From Tuned Molecular Quantum Similarity Measures: Prediction of the Corticosteroid-Binding Globulin Binding Affinity From a Steroid Family. *J. Chem. Inf. Comput. Sci.* **1999**, *39*, 333−344.

(57) Karelson, M.; Lobanov, V. S.; Katritzky, A. R. Quantum-Chemical Descriptors in QSAR/QSPR Studies. *Chem. Rev.* **1996**, *96*, 1027−1044.

(58) Turner, D. B.; Willett, P.; Ferguson, A. M.; Heritage, T. Evaluation of Novel Infrared Range Vibration-Based Decriptor (EVA) for QSAR Studies: 1. General Application. *J. Comput.-Aided Mol. Des.* **1997**, *11*, 409−422.

(59) Turner, D. B.; Willett, P. The EVA Spectral Descriptor. *Eur. J. Med. Chem.* **2000**, *35*, 365−375.

(60) Bursi, R.; Dao, T.; van Wijk, T.; de Gooyer, M.; Kellenbach, E.; Verwer, P. Comparative Spectra Analysis (CoSA): Spectra As Three-Dimensional Molecular Descriptors for the Prediction of Biological Activities. *J. Chem. Inf. Comput. Sci.* **1999**, *39*, 861−868.

(61) Tuppurainen, K.; Ruuskanen, J. Electronic Eigenvalue (EEVA): a New QSAR/QSPR Descriptor for Electronic Substituent Effects Based on Molecular Orbital Energies. A QSAR Approach to Ah Receptor Binding Affinity of Polychlorinated Biphenyls (PCBs), Dibenzo-p-Dioxins (PCDDs) and Dibenzofurans (PCDFs). *Chemosphere* **2000**, *41*, 843−848.

(62) Tuppurainen, K. EEVA (Electronic Eigenvalue): A New QSAR/QSPR Descriptor Based on Molecular Orbital Energies. *SAR QSAR Environ. Res.* **1999**, *10*, 39−46.

(63) Tuppurainen, K.; Viisas, M.; Laatikainen, R.; Peräkylä, M. Evaluation of Novel Electronic Eigenvalue (EEVA) Molecular Descriptor for QSAR/QSPR Studies: Validation Using a Benchmar Steroid Data Set. *J. Chem. Inf. Comput. Sci.* **2002**, *42*, 607−613.

(64) Asikainen, A. H.; Ruuskanen, J.; Tuppurainen, K. Performance of (Consensus) KNN QSAR for Predicting Estrogenic Activity in Large Diverse Set of Organic Compounds. *SAR QSAR Environ. Res.* **2004**, *15*, 19−32.

(65) Fontaine, F.; Pastor, M.; Sanz, F. Incorporating Molecular Shape into the Alignment-Free GRid-INdependent Descriptors. *J. Med. Chem.* **2004**, *47*, 2805−2815.

(66) Korhonen, S.-P.; Tuppurainen, K.; Laatikainen, R.; Peräkylä, M. FLUFF-BALL, A Template-Based Grid-Independent Superposition and QSAR Technique: Validation Using a Benchmark Steroid Data Set. *J. Chem. Inf. Comput. Sci.* **2003**, *43*, 1780−1793.

(67) Asikainen, A. H.; Ruuskanen, J.; Tuppurainen, K. Consensus KNN QSAR: A Versatile Method for Predicting the Estrogenic Activity of Organic Compounds In Silico. A Comparative Study With Five Estrogen Receptors and a Large, Diverse Set of Ligands. *Environ. Sci. Technol.* **2004**, *38*, 6730−6740.

(68) Halgren, T. A. Merck Molecular Force Field. I. Basis, Form, Scope, Parametrization, and Performance of MMFF94. *J. Comput. Chem.* **1996**, *17*, 490−519.

(69) Halgren, T. A. Merck Molecular Force Field. II. MMFF94 van der Waals and Electrostatic Parameters for Intermolecular Interactions. *J. Comput. Chem.* **1996**, *17*, 520−552.

(70) Halgren, T. A. Merck Molecular Force Field. III. Molecular Geometries and Vibrational Frequencies for MMFF94. *J. Comput. Chem.* **1996**, *17*, 553−586.

(71) Halgren, T. A. Merck Molecular Force Field. IV. Conformational Energies and Geometries for MMFF94. *J. Comput. Chem.* **1996**, *17*, 587−615.

(72) Halgren, T. A. Merck Molecular Force Field. V. Extension of MMFF94 Using Experimental Data, Additional Computational Data, and Empirical Rules. *J. Comput. Chem.* **1996**, *17*, 616−641.

(73) Sippl, W. Receptor-Based 3D QSAR Analysis of Estrogen Receptor Ligands − Merging the Accuracy of Receptor-Based Aligment With Computational Efficiency of Ligand-Based Methods. *J. Comput.-Aided Mol. Des.* **2000**, *14*, 559−572.
(74) Tong, W.; Perkins, R. QSAR Models for Binding of Estrogenic Compounds to Estrogen Receptor α and β Subtypes. *Endocrinology* **1997**, *138*, 4022−4025.
(75) Tong, W.; Perkins, R.; Strelitz, R.; Collantes, E. R.; Keenan, S.; Welsh, W. J.; Branham, W. S.; Sheehan, D. M. Quantitative Structure−Activity Relationships (QSARs) for Estrogen Binding to the Estrogen Receptor: Predictions Across Species. *Environ. Health Perspect.* **1997**, *105*, 1116−1124.
(76) Waller, C. L.; Oprea, T. I.; Chae, K.; Park, H.-K.; Korach, K. S.; Laws, S. C.; Wiese, T. E.; Kelce, W. R.; Grey, L. E. J. Ligand-Based Indentification of Environmental Estrogens. *Chem. Res. Toxicol.* **1996**, *9*, 1240−1248.
(77) Wolohan, P.; Reichert, D. E. CoMFA and Docking Study of Novel Estrogen Subtype Selective Ligands. *J. Comput.-Aided Mol. Des.* **2003**, *17*, 313−328.
(78) Kubinyi, H. Comparative Molecular Field Analysis (CoMFA). In *Encyclopedia of Computational Chemistry*; Wiley & Sons: 1998; pp 3001−3012.
(79) Tropsha, A.; Gramatica, P.; Gombar, V. K. The Importance on Being Earnest: Validation Is the Absolute Essential for Successful Application and Interpretation of QSPR Models. *Quant. Struct.−Act. Relat.* **2003**, *22*, 69−76.
(80) Cho, S. J.; Tropsha, A. Cross-Validated R2-Guided Region Selection for Comparative Molecular Field Analysis: A Simple Method to Achieve Consistent Results. *J. Med. Chem.* **1995**, *38*, 1060−1066.

CI050021I